Bioorganic & Medicinal Chemistry 17 (2009) 2695–2702

Contents lists available at ScienceDirect

Bioorganic & Medicinal Chemistry

journal homepage: www.elsevier.com/locate/bmc

Modified low molecular weight cyclic peptides as mimetics of BDNF with improved potency, proteolytic stability and transmembrane passage in vitro ☆

Jordan M. Fletcher, Richard A. Hughes *

The Department of Pharmacology, The University of Melbourne, Victoria 3010, Australia

ARTICLE INFO

Article history:
Received 3 October 2008
Revised 20 February 2009
Accepted 21 February 2009
Available online 4 March 2009

Keywords:
BDNF
Neurotrophin
Agonist
Antagonist
Neurotrophic factor
p75

ABSTRACT

We recently reported the development of the BDNF mimetic peptide cyclo-[dPAKKR] **1** which promotes the survival of cultured sensory neurons via a trkB independent mechanism [Fletcher, J. M.; Morton, C. M.; Zwar, R. A.; Murray, S. S.; O'Leary, P. D.; Hughes, R. A. *J. Biol. Chem.* **2008**, *283*, 33375]. In the present study we prepared a series of hydrophobically-modified analogues of **1** with an eye to improving its pharmacokinetic properties. Select members of this second generation of compounds showed improved biological activity, stability in plasma, and an ability to cross model biological membranes.

1. Introduction

BDNF is a member of the neurotrophin family of neurotrophic factors which also includes nerve growth factor (NGF), neurotrophin-3 (NT-3), and neurotrophin-4/5 (NT-4/5). Owing to their ability to potently promote the survival of a variety of neurons, neurotrophins are widely considered to hold potential for the treatment of a range of human neurodegenerative conditions. In this respect BDNF is particularly attractive, as it has been shown to promote the survival and/or prevent the degeneration of neuronal populations implicated in several such disease processes, including motor neurons (involved in amyotrophic lateral sclerosis (ALS)), populations of sensory neurons (sensory neuropathies), basal forebrain cholinergic neurons (Alzheimer's disease) and dopaminergic neurons of the substantia nigra (Parkinson's disease). More recently, it has also been demonstrated that BDNF likely plays a specific role in the aetiology of Huntington's disease (reviewed by Alberch et al.,[1]) giving further potential for therapies aimed at replacing BDNF or otherwise mimicking its actions in this condition.

The biological activity of BDNF and the other neurotrophins is mediated through interaction with two cell-surface receptors: members of the trk family of receptor tyrosine kinases, and the glycoprotein $p75^{NTR}$. The binding of a neurotrophin to the appropriate trk receptor (NGF binds to trkA, BDNF and NT-4/5 bind to trkB, NT-3 binds primarily to trkC) leads to homodimerisation of the receptor and subsequent autophosphorylation, resulting in the activation of multiple signalling pathways, including those leading to survival and differentiation. In contrast, $p75^{NTR}$ binds all the neurotrophins with similar low affinity ($K_D \approx 10^{-9}$ M). Although controversy still surrounds the exact role of $p75^{NTR}$ in mediating neurotrophin actions, there is a considerable body of evidence indicating that $p75^{NTR}$ is involved in regulating apoptosis, as well as modulating trk-related signalling. The ultimate consequence of neurotrophin activation of a trk member and $p75^{NTR}$ depends on the amounts and relative concentration of each receptor and other aspects of the context of their cellular presentation.[2,3]

Despite an abundance of promising pre-clinical data, BDNF has met with little success in the clinical setting. Indeed, in a phase III trial for the treatment of ALS, daily subcutaneous administration of BNDF was found to offer no clinical benefit.[4] Several reasons for this failure have been mooted, at the forefront of which centre concerns regarding the pharmacokinetic properties of the protein itself. For instance, BDNF has been shown to possess a plasma half life of just 1 min in the rat.[5] In order to circumvent these pharmacokinetic hurdles, our laboratory is focused on the development of BDNF functional mimetics that retain the desirable biological activity of BDNF, but under the guise of a small molecule possessing improved pharmacokinetic properties.

To generate peptides capable of mimicking BDNF's biological activity, we have in earlier studies used the 3D structure of BDNF

☆ This work was funded by the National Health and Medical Research Council of Australia.

* Corresponding author. Tel.: +61 3 8344 8604; fax: +61 3 8344 0241.
E-mail address: rahughes@unimelb.edu.au (R.A. Hughes).

0968-0896/$ - see front matter Crown Copyright © 2009 Published by Elsevier Ltd. All rights reserved.
doi:10.1016/j.bmc.2009.02.053

1

Figure 1. The lead compound **1**.

as a template for the design of conformationally-constrained peptides as structural mimetics of the regions of BDNF which—by way of site directed mutagenesis studies[6]—have been implicated in receptor binding. Our previous studies have yielded: (I) monomeric-monocyclic peptides based on a single solvent-exposed loop (loop 1, 2 or 4) of BDNF as putative TrkB ligands which behave as inhibitors of BDNF;[7,8] (II) Dimeric-bicyclic and dimeric-tricyclic peptides based on the two loop 2 regions of BDNF that are putative trkB ligands and behave as highly-potent partial BDNF-like agonists;[9] and most recently (III) a head-to-tail cyclic pentapeptide (**1**; Fig. 1),[10] which consists of the $p75^{NTR}$-binding tripeptide motif (Lys-Lys-Arg)[11] present on loop 4 of BDNF constrained by a dPro-Ala linker. Unlike other monomeric BDNF loop mimetics we have examined that act as BDNF antagonists, pentapeptide **1** was found act as a BDNF-like agonist and promote the survival of chick sensory neurons in vitro. Consistent with its design as a $p75^{NTR}$-binding mimetic, we found that pentapeptide **1** was unable to activate trkB. We further found by NMR studies that pentapeptide **1** adopts a highly defined backbone conformation in solution, and is highly stable to proteolytic degradation by plasma in vitro. These findings, together with the low molecular weight of pentapeptide **1**, render it worthy of further examination as a lead compound for the development of a clinically useful BDNF-like neurotrophic drug.

In the present study we have sought to further exploit this potential of pentapeptide **1** by designing a series of hydrophobic analogues of **1** and examining (I) their ability to promote neuronal survival; (II) their stability in plasma; and (III) their ability to cross cell membranes.

2. Results

2.1. Synthesis

A total of 7 peptides were generated in the present study: the lead compound peptide **1** (previously reported[10]); the Phe and Nle substituted derivatives **2** and **3**; the series of alkyl amide-substituted analogues **5**, **6**, and **7**, as well as their un-alkylated parent the Lys-substituted peptide **4**. The structures of these compounds are presented in Table 1.

Preparation of the head-to-tail cyclic pentapeptides **1**–**4** (Scheme 1) was facile. The linear precursors were prepared by solid-phase assembly on 2-chlorotrityl resin, followed by mild acid cleavage from the resin, leaving side-chain protecting groups intact. The solution-phase head-to-tail cyclisation of the protected precursors proceeded smoothly, presumably owing to the dPro residue conferring a favourable turn. All cyclisations were monitored by RPHPLC and were complete within an hour and in near quantitative yield. After removal of side-chain protection, the cyclic pentapeptides were purified to ~95%, and their identity confirmed by mass spectrometry.

Synthesis of the three alkyl amide-substituted analogues (**5**–**7**) made use of a mixed lysine protection strategy employing Lys^{Boc} and Lys^{ivDde} (Scheme 2). The initial solid-phase assembly, cleavage from the resin, and cyclisation proceeded without incident, yielding the fully-protected cyclic derivative **12**. ivDde protection of one of the Lys residues in **12** was removed using 2% hydrazine to give **13**; MeOH was used as a solvent rather than the more commonly used DMF to aid work-up from this solution-phase reaction.

Table 1
Structure of peptides and summary of neuronal survival data

Peptide	Structure	pEC_{20BDNF}[a]	Maximum observed % normalised neuronal survival
1	dPAKKR	7.3	67.7 ± 2.8%[b]
2	dPFKKR	5.3	21.8 ± 7.2%
3	dPNIeKKR	6.2	36.2 ± 6.3%
4	dPKKKR	7.5	60.9 ± 5.4%
5	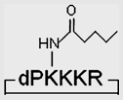	7.7	39.4 ± 7.5%
6	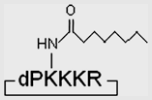	7.5	38.7 ± 7.4%
7	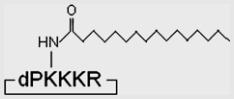	9.1	49.4 ± 12.4%

[a] % Normalised maximal response and pEC_{20BDNF} values described for peptide **7** as determined from the concentration–response curved generated over the concentration range 1×10^{-10} to 1×10^{-5} M (Fig. 2 Panel C).

[b] The maximum% normalised neuronal survival for **1** occurred at 10^{-4} M—a concentration at which no peptide in the current study was examined. In the *absence* of this data point, the maximum observed response for peptide **1** was 37.3 ± 2.4%.

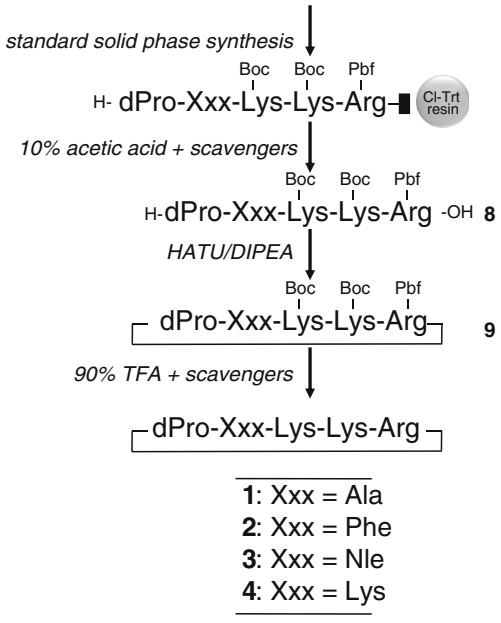

Scheme 1. Synthesis of cyclic pentapeptides **1**–**4**.

The removal of ivDde was monitored by RPHPLC and, although more sluggish than if the reaction had been carried out in DMF, proceeded cleanly and to completion in ~2 h. Subsequent HATU-mediated coupling of fatty acids to the lysine side-chain amino function of **13** proceeded rapidly, with all couplings complete well inside 20 min, as shown by RPHPLC monitoring. Following cleavage of side-chain protection, the alkyl amide-substituted peptides

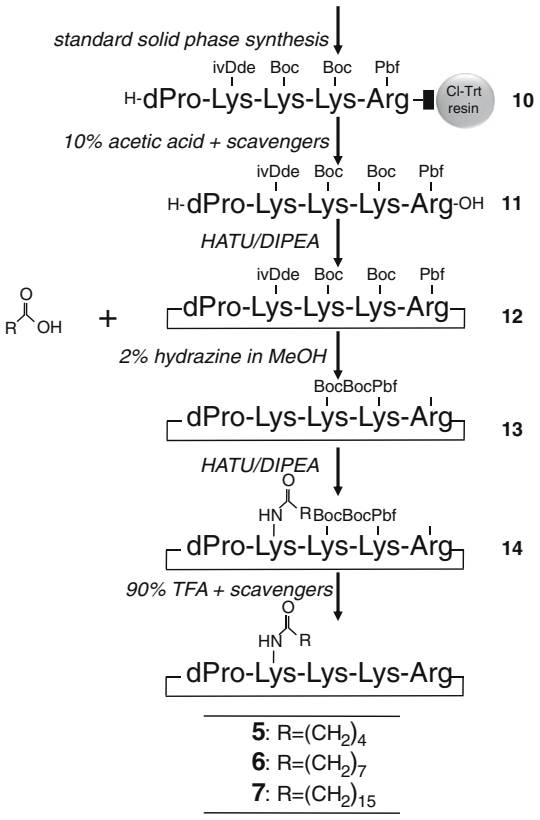

Scheme 2. Synthesis of alkyl amide-substituted cyclic pentapeptides **5**–**7**.

5–**7** were purified to over ~95% purity, and their identity confirmed by ESI-MS.

2.2. Neuronal survival

When examined in primary cultures of embryonic chick DRG sensory neurons, all peptides produced a concentration-dependent increase in neuronal survival (Fig. 2). The maximum observed level of survival was varied, but in most cases (with the exception of **2**) proved significantly different to negative controls ($p < 0.05$; ANOVA, post-hoc Dunnett's test; $n = 3, 4$). Since the concentration–response curves for most peptides did not attain a stable plateau of maximal response, pEC_{50} values could not be determined. Instead we opted to introduce the parameter pEC_{20BDNF} (defined earlier) as a means of quantifying (and comparing) the peptides' relative potency. A summary of pEC_{20BDNF} values and maximum observed responses is provided in Table 1. For the purpose of comparison, sensory neuron survival data previously described[10] for the lead compound **1** is also presented in this communication.

The most potent compound generated in this study was the longest-chain fatty alkyl amide-substituted pentapeptide **7**. When added to cultures of sensory neurons, **7** produced a concentration-dependent increase in neuronal survival (Fig. 2; Panel B) with a potency that exceeded our initial expectations (based primarily on the activity of **1**). Indeed, in our initial experiments (i.e., from 1×10^{-8} to 1×10^{-5} M) the EC_{20BDNF} of **7** could not be determined as even at the lowest concentration tested (1×10^{-8}) it gave a % normalised neuronal survival of 28.4 ± 4.6% (i.e., >20%). Thus, **7** was re-examined from 1×10^{-10} to 1×10^{-5} M where it was found to produce a maximal survival effect of (49.4 ± 12.4%, which is significantly different to negative controls ($p < 0.05$; ANOVA, post-hoc Dunnett's test; $n = 3$)), and a pEC_{20BDNF} of 9.1 (Table 1), rendering it unequivocally the most potent compound produced by the current study. For the purpose of comparison, Figure 2, Panel C shows the concentration response curve for **7** plotted against the lead compound from this study **1** (previously reported[10]).

Whilst peptide **7** was the most potent peptide produced, other compounds also exhibited pEC_{20BDNF} values greater than 7 (see Table 1). Indeed, peptide **4** ($pEC_{20BDNF} = 7.5$), peptide **5** ($pEC_{20BDNF} = 7.7$) and peptide **6** ($pEC_{20BDNF} = 7.5$) were all found to be of approximately equal potency to the lead compound **1** ($pEC_{20BDNF} = 7.3$). All remaining peptides were less potent than **1**.

2.3. Stability in plasma

Pentapeptide **1** and the alkyl amide-substituted peptide **6** were examined in an in vitro model of stability in plasma. In addition, substance P (an 11 amino acid peptide known to be rapidly degraded in plasma) was also tested to confirm that our experimental protocol was a valid means of determining stability. In our hands, substance P exhibited a half life of 22 ± 9 min, which was in good accordance with previously published in vivo results in humans ($t_{1/2} = 24$ min[12]). In contrast, peptides **1** and **6** were found to be remarkably stable. Figure 3 shows the % normalised concentration (in mouse plasma) of each of these three peptides over the 24 h period of incubation. Compound **1** was completely resistant to degradation with no loss of peptide observed over the duration of the assay, whilst only a small amount (~20%) of **6** was lost over the 24 h time period. This stability precluded a robust estimation of plasma half life, but it is clear that the half life of both **1** and **6** in the mouse plasma system is very much greater than 24 h. Unfortunately, the stability of the peptide showing the greatest biological

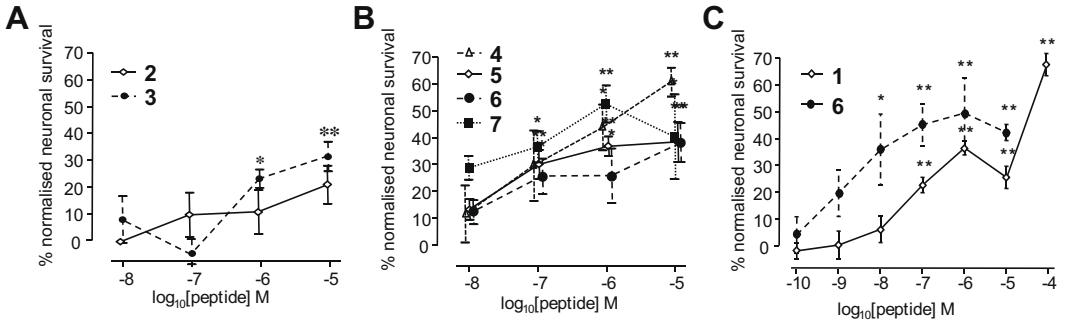

Figure 2. Concentration–response curves for peptides prepared in this study. Peptides were examined in primary cultures of chick sensory neurons. Surviving neurons in treatment wells were counted after 48 h. Data was normalised between BDNF positive (100%) and negative (0%) controls ($^{*}p < 0.05$; $^{**}p < 0.01$; $n = 3$–4 in triplicate). *Panel A*: Cyclic pentapeptides **2** and **3**; *Panel B*: The alkyl amide-substituted series **5**, **6**, and **7** as well as their un-alkylated 'parent' **4**; *Panel C*: Re-examination of the highly-potent peptide **7** from 1×10^{-10} to 1×10^{-5} M, plotted against the lead compound **1** (previously published[10]).

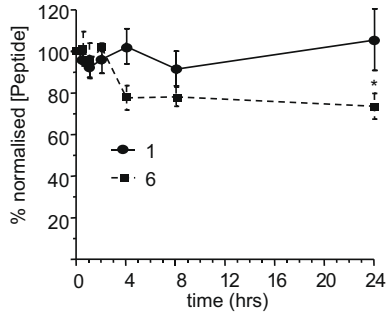

Figure 3. Time course for the stability of peptides **1** and **6** in mouse plasma.

activity (peptide **7**) could not be determined, as this peptide co-eluted with unprecipitated proteins in the HPLC assay used. Nevertheless, given the extreme stability of peptides 1 and 6 under the conditions used, we would expect peptide 7 to also be stable in plasma in vitro.

2.4. Membrane permeability

Caco-2 cells were cultivated as monolayers for 24–25 days on permeable supports. After this period, monolayer integrity was confirmed by measurement of the TEER across each monolayer, as well as by the passage of ^{14}C-mannitol across control monolayers. Across all monolayers used, TEER averaged 280 Ω cm^2 and showed a standard deviation of 35.6 Ω cm^2, figures which sit comfortably amongst previously published observations (e.g.,[13,14]). Two monolayers found to possess a TEER of less than 200 Ω cm^2 were discarded. The passage of ^{14}C-mannitol across a total of 10 controls was also consistent with the presence of intact monolayers—the P_{app} of ^{14}C-mannitol was calculated to be $4.36 \pm 0.59 \times 10^{-7}$ cm s^{-1} in line with previous reports. The importance of this parameter is discussed later.

All peptides prepared in the present study were examined in the Caco-2 membrane permeability assay. Unfortunately however, experimental difficulties hampered our efforts to successfully quantify the concentration of several peptides in samples collected during experiment. There were three primary reasons for this: (A) Peptides bound/associated with the BSA present in Caco-2 samples; (B) Peptides (particularly **1** and **4**) adhered poorly to the LCMS reverse-phase column; and (C) Peptides appeared to yield inconsistent and not concentration-dependant species by mass spectrometry. An extensive and varied array of techniques (not shown) was trialled to overcome these problems. The most successful method—and the method that was ultimately used—involved post assay acetylation of the peptide and subsequent quantification by LCMS of the single, bis-acetylated species that formed. In this manner, successful analysis was achieved for 4 of the 8 peptides examined (**1**, **3**, **5**, and **6**). Table 2 shows the P_{app} of these peptides as well as ^{14}C-mannitol controls. We were unable to obtain a suitable signal for peptide 7, apparently due to its very high degree of retention a wide range of LC conditions that we examined (data not shown). A comprehensive description for the gathering and analysis of results from Caco-2 experiments is provided as Supplementary data, available from the Web-based edition of this Journal.

Table 2
P_{app} for peptides **1**, **3**, **5**, and **6** as well as the ^{14}C-mannitol control

Compound	P_{app} (cm s^{-1})	n
1	$6.42 \pm 0.35 \times 10^{-7}$	4
3	$2.88 \pm 0.73 \times 10^{-7}$	3
5	$9.29 \pm 1.27 \times 10^{-7}$	3
6	$9.22 \pm 2.26 \times 10^{-7}$	4
^{14}C-mannitol	$4.36 \pm 0.59 \times 10^{-7}$	10

Results are shown as mean ± SEM from 3 to 4 monolayers for each of the peptides, and 10 monolayers for ^{14}C-mannitol.

3. Discussion

The development of the putative p75^{NTR} ligand 1 was recently described by our laboratory.[10] In the present study, we sought to develop analogues of **1** that possess drug-like properties, including: (i) stability in plasma; (ii) a capacity to penetrate biological membranes; and (iii) high potency. Substantial steps towards these goals were achieved.

There are a variety of different strategies available for improving the membrane permeability of a given peptide.[15,16] Techniques which are commonly employed include the attachment of lypophilic substituents,[17,18] or the conjugation of moieties that enable the peptide to exploit endogenous transport mechanisms, such as so-called 'trojan peptides',[19] or small non-peptidic carriers, such as β-D-glucose.[20,21] In the present study we prepared and examined analogues of **1** substituted with fatty acids of varying length.

The Ala residue of pentapeptide **1** was chosen as the site for hydrophobic modification. We reasoned that this residue would be most amenable to modification without adversely affecting the biological activity of **1**, given that we had previously demonstrated that the Lys-Lys-Arg tribasic motif was likely to be of functional importance, and that the DPro residue plays a key a structural role.[10] As it transpired, the analogues with modifications at this position did show quite marked differences in neuronal survival activity, with compounds showing both lesser and greater potency and maximal neuronal survival activity than the parent **1**, suggesting that this position is not as functionally 'silent' as we anticipated.

The most potent compound prepared in this study was the longest-chain alkyl amide-substituted derivative **7**, which exhibited a pEC_{20BDNF} of 9.1 (Fig. 2, Panels b and c; Table 1), making it approximately 25-fold more potent than the next most potent compound prepared in this study (**5**; $pEC_{20BDNF} = 7.7$), and over 60-fold more potent than the lead compound (**1**; $pEC_{20BDNF} = 7.3$). Such an increase in potency following addition of a long alkyl chain to a peptide is not without precedent, having been reported with fatty alkyl amide-substituted analogues of an α-melanotropin-derived cyclic hexapeptide,[22,23] and of α-melanotropin-derived cyclic tetrapeptides.[24] Similar results have also been shown for proteins—for example, conjugation of fatty acids to the N-terminus of sonic hedgehog leads to a 100-fold increase in the potency.[25] The mechanism by which hydrophobic modification of peptides and proteins can give rise to an increase in potency is not well understood. One elegant explanation however has been put forward by Schwyzer and colleagues[26,27] who suggested that membrane lipids can act as a 'catalyst' for receptor binding, whereby the hydrophobic compound associates firstly with the cellular membrane, before going on to bind its receptor, leading to a higher local concentration at the receptor site. By restricting the dispersion of the compound away from its site of action, derivatives of **1** that exhibit a strong membrane interaction might also be of value following in vivo administration. Such a mode of action is thought to be utilized by the lypophillic, long acting β-adrenoceptor agonists formeterol and salmeterol used in the treatment of asthma.[28] Whether this mechanism is responsible for the high potency of the hydrophobic peptide **7** remains an area for future study.

With the aid of a post acetylation derivitisation step, it was possible to establish an LCMS-based assay of suitable sensitivity to allow the study of several of the hydrophobic compounds from this

study in a membrane passage system using Caco-2 cells. The Caco-2 cell monolayer model is the most widely used in vitro method for examining membrane passage of compounds, and subsequently as a predictor for their absorption in vivo following oral administration. Despite this, relating P_{app} in this assay for a given compound to its likely in vivo absorption remains a difficult prospect. Several groups[29–32] have reported very strong individual correlations between P_{app} across Caco-2 monolayers and in vivo absorption across intestinal epithelium in vivo. However, as noted by Artursson and colleagues[33] the correlation between studies is poor. Thus, if the data from these four papers is plotted on a common set of axes, the individual correlation curves are shifted left or right relative to one another, (see Fig. 4, Panel A). The prevailing thought is that these disparities arise because of differences between the Caco-2 cell lines used in each laboratory. Indeed, Caco-2 cell lines are heterogeneous by nature and, given that cells of passage number 50–100 are routinely used, it is more than likely that subtle variances in routine cell handling techniques gives rise to different selection pressures, and subsequently, to marginally different Caco-2 cell lines over time. With this in mind, caution needs to be exercised when comparing results from Caco-2 studies from different laboratories.

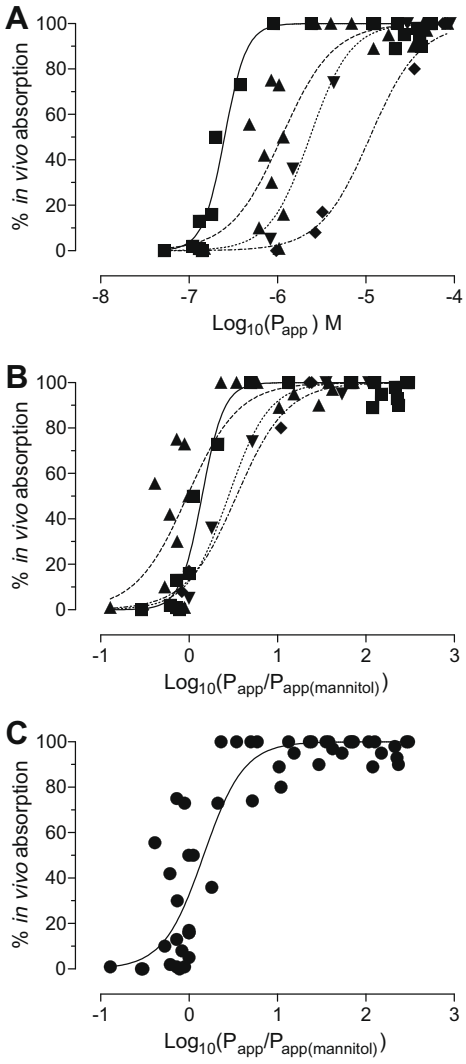

Figure 4. Analysis of literature correlations between Papp across Caco-2 monolayers and absorbance across the intestinal epithelium in vivo. Data presented is compiled from 4 sources: (■[30]; ♦[31]; ▼[32]; ▲[29]). Two apparent outliers have been excluded from the analysis: amoxicillin[29]; and PEG-900.[31] *Panel A*: Correlation between $Log_{10}(P_{app})$ and in vivo absorption as reported in the 4 selected studies. A plot similar to this has been previously published,[40] however, in this figure, the more recent contribution from Grès and co-workers[29] has also been included. *Panel B*: The effect of standardising each set of data to ^{14}C-mannitol. The plot was prepared by dividing the P_{app} of each compound in each study by the P_{app} of ^{14}C-mannitol observed in that particular study. *Panel C*: Combined, normalised-to-mannitol data from the 4 studies. A Boltzman sigmoidal curve is fitted.

Of particular concern to us in our study was the fact that using this published information, it would not possible to make a definitive statement about the likely in vivo absorption of the compounds from their P_{app} we had determined for them, as the prediction we would make would be entirely dependent on which set of published data we chose to use. For instance, if we consider peptide **1** (P_{app} of $6.42 \pm 0.35 \times 10^{-7}$ cm s^{-1}), the correlation provided by Rubas and colleagues[31] indicates that **1** would be unlikely to cross the intestinal epithelium in vivo, while the correlation from Artursson's group[30] suggests that compounds with a P_{app} similar to pentapeptide **1** would be almost 100% absorbed following oral administration in vivo (see Fig. 4, Panel A).

Faced with this situation, we sought a way to standardise these literature studies with a view to deriving a 'consensus' relationship between P_{app} across Caco-2 monolayers and absorption in vivo following oral administration. ^{14}C-mannitol is used almost ubiquitously in Caco-2 assays as a control for monolayer integrity, and thus serves as a potential reference compound to allow standardisation of data from different sources. Indeed, if the data in Figure 4 Panel A are expressed relative to mannitol, (by dividing the P_{app} observed for each compound in each study by the P_{app} of mannitol from that given study), a much more consistent picture emerges (Fig. 4, Panel B), with greatly reduced variation between the correlations established by the four groups. With the sets of data standardised, the data presented by each of the four groups can be combined and plotted as normalised-to-mannitol P_{app} versus in vivo absorption (Fig. 4, Panel C; $R^2 = 0.81$ for Boltzmann sigmoidal curve fitted to normalised combined data). To our knowledge, the manipulation of literature data in this fashion has not been previously described, and offers a vastly improved scope for predicting the in vivo absorption of a compound across the gut epithelium from its P_{app} across Caco-2 monolayers, by allowing the comparison of results from Caco-2 experiment from different laboratories.

With this refined method for analysing and comparing Caco-2 membrane permeability data, the correlation between in vivo absorption and standardised P_{app} (as depicted in Fig. 4, Panel C) could be used as a basis for making predictions about the likely in vivo absorption of the compounds investigated in the present study (see Table 3). Thus, by interpolation from Figure 4, Panel C, it can be predicted that following oral administration of the lead compound, peptide **1**, approximately 40% of the administered dose would be absorbed across the intestinal epithelium. The two fatty alkyl amide-substituted derivatives **5**, and **6** would be absorbed a greater extent, with 60% of the administered dose predicted to cross the intestinal epithelium. In contrast, the norleucine-substituted derivative **3** is predicted to show limited absorption at approximately 10%. These predictions await experimental verification.

Table 3
P_{app}, $Log_{10}(P_{app}$ normalised to mannitol), and the predicted in vivo absorption across the intestinal epithelium for peptides **1**, **3**, **5**, and **6**

	P_{app} (cm s^{-1})	$Log_{10}\left(\frac{P_{app}}{P_{app(mann)}}\right)$	Predicted in vivo abs. (%)
1	$6.42 \pm 0.35 \times 10^{-7}$	0.16	≈40
3	$2.88 \pm 0.73 \times 10^{-7}$	−0.18	≈10
5	$9.29 \pm 1.27 \times 10^{-7}$	0.33	≈60
6	$9.22 \pm 2.26 \times 10^{-7}$	0.33	≈60

In vivo absorption was predicted using the relationship between in vivo absorption and normalised P_{app} depicted in Figure 4, Panel C.

All of the compounds examined showed very high stability in mouse plasma in vitro, exhibiting little or no degradation over the 24 h period studied. Given that effective absorption following oral administration of a drug requires both good passage across cell membranes (i.e., the property addressed in the Caco-2 experiments) and good metabolic stability (to reduce the effects of presystemic—gut and hepatic—metabolism), peptide **1** and the lipidated analogues presented in this study clearly warrant further pre-clinical investigation for their effects on models of neuronal degeneration in vivo, including after oral administration.

4. Conclusion

In this study we have described the development of hydrophobically-modified analogues of our neuronal survival-promoting cyclic pentapeptide **1**. We found peptides which were: (I) highly-potent promoters of neuronal survival; (II) stable in plasma; and (III) likely to possess a moderate level of intestinal absorption. We hope to use the results generated in this study as a basis for producing further generations of compound, and to examine them in in vivo animal models of neurodegenerative disease.

5. Experimental

5.1. Materials

Fluorenylmethoxycarbonyl (Fmoc)-protected amino acids, 2-(1*H*-9-azabenzotriazole-1-yl)-1,1,3,3-tetramethyluronium hexafluorophophate (HATU), 2-(1*H*-benzotriazol-1-yl)-1,1,3,3-tetramethyluronium hexafluorophophate (HBTU), diisopropy lethylamine (DIPEA), *N*,*N*-dimethylformamide (DMF), piperidine, trifluoroacetic acid (TFA) and substance P: Auspep, Parkville, Vic., Australia; 2-chlorotrityl resin: Novabiochem, Darmstadt, Germany; 2,3,4,6-tetra-*O*-acetyl-D-glucopyranose: Rose Scientific, Edmonton, Alberta, Canada; Recombinant human BDNF: Research and Diagnostic Systems, Minneapolis, USA; fertilised chicken eggs: Research Poultry, Research, Vic, Australia; trypsin: Worthington, Freehold, NJ, USA; horse serum, penicillin and streptomycin: CSL Parkville, Vic., Australia; L-15 medium: GibcoBRL, Grand Island, NY, USA; Poly-DL-ornithine: Sigma, St. Louis, USA; laminin: Collaborative Biomedical Products, Bedford, MA, USA; Nunclon 10 cm-diameter tissue culture dish: Nalge Nunc International (Roskilde, Denmark); 48-well tissue culture plates: Becton Dickinson (Franklin Lakes, NJ, USA); all other reagents: Sigma, Castle Hill, NSW, Australia.

5.2. Peptide synthesis

5.2.1. Solid-phase assembly

All peptides were assembled using a Protein Technologies™ PS3 Automated Peptide Synthesiser (Rainin Instrument Company Inc.; Woburn MA, USA) using standard batch-reaction, Fmoc solid-phase techniques (for review, see Chan and White[34]). Fmoc-protected amino acids (3 equiv) were coupled in the presence of HBTU (3 equiv) and DIPEA (4.5 equiv) in DMF (30 min), while removal of Fmoc-protecting groups was achieved by treatment with 20% piperidine in DMF (20 min). All reactions were performed under nitrogen. The cycle of coupling and deprotection reactions (interspaced with washings; DMF, 5 × 5 mL) were continued until the linear peptide sequence was complete. The side-chain protecting groups used were Arg: 2,4,6,7-pentamethyldihydrobenzofuran-5-sulfonyl (Pbf); and Lys: *t*-butoxycarbonyl (Boc), or 1(4,4-dimethyl-2,6-dioxocyclohex-1-ylidene)-3-methylbutyl (ivDde) as appropriate.

5.2.2. Resin cleavage

Peptides were cleaved from 2-chlorotrityl chloride resin in their side-chain protected form by treatment with DCM/trifluoroethanol(TFE)/CH_3COOH (8:1:1, 10 mL). After 30 min resin was removed by filtration, and the peptide-containing solution concentrated under reduced pressure. H_2O/MeCN (3:1, ~50 mL) was then added to the residue and the solution lyophilised. The linear protected pentapeptides were characterised by ESI-MS and used in subsequent reactions without purification.

5.2.3. Cyclisation

Crude linear peptides were dissolved in DCM (to give a peptide concentration of 0.5 mg/mL) to which a pre-mixed solution of HATU (2 equiv) and DIPEA (3 equiv) in DMF (~500 μL) was added. The time-course of the ensuing cyclisation was monitored by RPHPLC. Once the reaction was complete, DCM was removed under reduced pressure (37 °C, ~30 min), H_2O/MeCN (3:1, ~50 mL) added to the residue, and the solution lyophilised. The cyclic, fully-protected peptides were purified by RPHPLC and analysed by ESI-MS.

5.2.4. Lys^{ivDde} deprotection

ivDde was selectively removed from one of the the Lys side-chains of peptide **12** (40 mg) by treating the peptide with 2% hydrazine in MeOH (mL). The reaction was monitored by RPHPLC and after 2 h, the reaction mixture was diluted with water (~200 mL), concentrated under reduced pressure (50 °C; ~2 h), and lyophilised to give the crude partially-deprotected cyclic peptide **13**.

5.2.5. Solution-phase coupling of fatty acids

Three fully-protected, fatty alkyl amide-substituted cyclic pentapeptides were prepared by coupling the linear-chain fatty acids (valeric, octanoic, or palmitic acids, respectively) to the side-chain amino group of the partially protected derivative **13**. In each experiment, a solution of peptide **13** (5 mg/mL) and fatty acid (3 equiv) in DMF was prepared, to which a pre-dissolved mixture of HATU (2 equiv) and DIPEA (3 equiv) was added. The progress of the reactions was monitored by RPHPLC. Once complete, the reaction mixtures were diluted with H_2O/MeCN and the peptide-containing solutions lyophilised.

5.2.6. Side-chain deprotection

Boc and Pbf side-chain protecting groups were cleaved from cyclic peptides by treatment with TFA/EDT/H_2O (18:1:1; 5 mL) for 90 min. Reaction mixtures were then diluted in ice-cold Et_2O (50 mL), and peptides extracted three times with water (3 × 50 mL). Aqueous phases were then pooled and washed three times with Et_2O. Residual Et_2O was removed under reduced pressure (37 °C, ~30 min) and the peptide-containing solutions lyophilised. Products were purified by RPHPLC and characterised by ESI-MS. Peptide **2**: $m/z_{obs.}$ 657.8, $[M+H]^+_{calcd}$ 657.4. Peptide **3**: $m/z_{obs.}$ 623.7, $[M+H]^+_{calcd}$ 623.4. Peptide **4**: $m/z_{obs.}$ 638.6, $[M+H]^+_{calcd}$ 638.5. Peptide **5**: $m/z_{obs.}$ 722.7, $[M+H]^+_{calcd}$ 722.5. Peptide **6**: $m/z_{obs.}$ 764.9, $[M+H]^+_{calcd}$ 764.5. Peptide **7**: $m/z_{obs.}$ 876.0, $[M+H]^+_{calcd}$ 876.5.

5.3. Sensory neuron survival assay

The ability of synthetic peptides to promote neuronal survival was assessed in primary cultures of dorsal root ganglion (DRG) sensory neurons obtained from embryonic chicks using the method previously described by our laboratory,[7,9] which is based on the protocol first described by Barde and co-workers.[35] Peptides were examined in $\log_{10}$ increments over the following ranges: Peptide **1**: 1×10^{-10} to 1×10^{-5} M); peptides **2**–**6**: 1×10^{-8} to 1×10^{-5} M; peptide **7**: 1×10^{-8} to 1×10^{-5} M as well as from 1×10^{-10} to

1×10^{-5} M. Experiments were performed in triplicate, a total of three or four times. Statistical analysis was performed using GraphPad Prism™ software (version 4.0; GRAPHPAD Software Inc.). For each experiment, data from triplicate well counts were averaged and normalised to BDNF positive (set to 100%) and negative (set to 0%) controls. Before grouping data from individual experiments, parametric one-way analysis of variance (ANOVA) was carried out to ensure variation of sample means between experiments was not significant. Grouped data was then expressed as mean ± standard error of the mean (SEM). One-way ANOVA, followed by post-hoc Dunnett's tests[36] were used to assess significant differences in neuronal survival between peptide treatments and BDNF-treated positive controls. Pairs of concentration–response curves were tested for significant difference by one-way ANOVA followed by post-hoc Bonferroni's multiple comparisons test.[37] Data was deemed to be significantly different to controls when p values were determined to be less than 0.05. For the purpose of comparing peptide potency we used the parameter pEC_{20BDNF}—which we define here as the negative $\log_{10}$ of the concentration of each peptide that elicits a % normalised neuronal survival response equivalent to 20% of that observed for BDNF positive controls.

5.4. Plasma stability assay

Peptides (0.2 mg) were incubated at 37 °C in a solution of plasma prepared from a single mouse (50% in PBS, 200 μL) in a siliconised 1.5 mL centrifuge tube. 4-Isopropylbenzyl alcohol (0.05% (v/v)) was added as an internal standard,[38] and the time-course of peptide degradation monitored by RPHPLC. At the final time point (24 h) the peak of interest was collected and the fraction analysed by mass spectrometry to rule out the possibility of degradation having occurred without a concomitant shift in RPHPLC retention time. Samples were prepared for analysis as follows: At each time point, an aliquot (10 μL) was removed from the peptide/plasma solution and placed immediately on ice. Each aliquot was then treated with L-lysine monohydrochloride (1000 equiv in 10 μL) to displace the peptide from possible plasma protein binding[10], and MeCN (60 μL) causing plasma proteins to precipitate from solution. Each aliquot was then centrifuged (4 °C, 10 min, 10,000 rpm) and the supernatant (60 μL) collected and transferred to a second 1.5 mL tube and diluted with water (100 μL). Samples were then loaded onto a C_{18} 'Rocket' column (Alltech™) and eluted using a linear gradient ranging from 100% solution A (0.1% TFA in H_2O) to 100% solution B (0.1% TFA in MeCN) over 16 min. The amount of peptide present at each time point was quantified as the 'area under the curve' for each compound eluted. Integrated peak areas for peptides were then expressed as a ratio of the internal standard (4-isopropylbenzyl alcohol; 0.05% (v/v)), before being expressed as a percentage of the ratio obtained at $t = 0$. Each experiment was performed three times. Before grouping of data from each experiment, parametric one-way analysis of variance (ANOVA) was carried out to ensure variation of sample means between experiments was not statistically significant. Grouped data was then expressed as mean ± standard error of the mean (SEM) and plotted against time.

5.5. Membrane permeability experiments

Peptides were examined for their ability to penetrate biological membranes using the so-called 'Caco-2 model' of membrane passage.[33] Experiments were based on those previously described.[30] In brief, monolayers were prepared by seeding Caco-2 cells (passage 82–96) onto Transwell™ polycarbonate membrane supports (0.45 μm pore size, 1.13 cm^2) and cultivated for 24–25 days. Monolayer integrity (i.e., tight junction formation) was confirmed by measurement of trans-epithelial electrical resistance (TEER) across each monolayer, and by measuring the passage of ^{14}C-mannitol across control monolayers. Transport studies were performed by adding peptide (200 μM in 400 μL HBSS) to the apical (inner) chamber, and then measuring its accumulation in the basolateral (outer) chamber (containing 1.5 mL HBSS with 30 g/L BSA (as recommended by[39]). At 30 min time points, for 150 min, 1 mL samples were removed from each basolateral compartment and replenished with fresh buffer. Each sample was then prepared for LCMS analysis as follows: (i) 250 μL of the peptide-containing solution was removed to a fresh 1.5 mL Clear-View® siliconized polypropylene tube; (ii) Peptides (and presumably BSA) were acetylated by the addition of triethyl amine (25 μL) and acetic anhydride (12.5 μL) at room temperature for 1 h; (iii) The acetylation reaction mixture was diluted with 1 mL of water and lyophilised; (iv) Dried, acetylated peptide-containing samples were redissolved in 2% aqueous TFA (250 μL), sonicated (10 min) and placed on ice (10 min); (v) Samples were then centrifuged (10,000 RPM, 10 min) causing undissolved, acetylated BSA adducts to collect as a solid pellet; (vi) 200 μL of supernatant was removed and the presence of the single, bis-acetylated peptide species analysed by LCMS.

Full experimental details of membrane permeability experiments are provided in the Supplementary data and are available on the Web-based edition of this Journal.

Acknowledgments

J.M.F. was the recipient of a Melbourne Research Scholarship. We would like to thank Dr. Colin House for assistance with LCMS analysis.

Supplementary data

Supplementary data associated with this article can be found, in the online version, at doi:10.1016/j.bmc.2009.02.053.

References and notes

1. Alberch, J.; Perez-Navarro, E.; Canals, J. M. *Prog. Brain Res.* **2004**, *146*, 195.
2. Huang, E. J.; Reichardt, L. F. *Annu. Rev. Biochem.* **2003**, *72*, 609.
3. Gentry, J. J.; Barker, P. A.; Carter, B. D. *Prog. Brain Res.* **2004**, *146*, 25.
4. The BDNF Study Group (Phase III). *Neurology* **1999,** *52*, 1427.
5. Poduslo, J. F.; Curran, G. L. *Brain Res. Mol. Brain Res.* **1996**, *36*, 280.
6. Ibanez, C. F. *J. Neurobiol.* **1994**, *25*, 1349.
7. O'Leary, P. D.; Hughes, R. A. *J. Neurochem.* **1998**, *70*, 1712.
8. Fletcher, J. M.; Hughes, R. A. *J. Pept. Sci.* **2006**, *12*, 515.
9. O'Leary, P. D.; Hughes, R. A. *J. Biol. Chem.* **2003**, *278*, 25738.
10. Fletcher, J. M.; Morton, C. M.; Zwar, R. A.; Murray, S. S.; O'Leary, P. D.; Hughes, R. A. *J. Biol. Chem.* **2008**, *283*, 33375.
11. Ryden, M.; Murray-Rust, J.; Glass, D.; Ilag, L. L.; Trupp, M.; Yancopoulos, G. D.; McDonald, N. Q.; Ibanez, C. F. *EMBO J.* **1995**, *14*, 1979.
12. Berger, H.; Fechner, K.; Albrecht, E.; Niedrich, H. *Biochem. Pharmacol.* **1979**, *28*, 3173.
13. Vermeirssen, V.; Deplancke, B.; Tappenden, K. A.; Van Camp, J.; Gaskins, H. R.; Verstraete, W. *J. Pept. Sci.* **2002**, *8*, 95.
14. Lindmark, T.; Kimura, Y.; Artursson, P. *J. Pharmacol. Exp. Ther.* **1998**, *284*, 362.
15. Witt, K. A.; Gillespie, T. J.; Huber, J. D.; Egleton, R. D.; Davis, T. P. *Peptides* **2001**, *22*, 2329.
16. Adessi, C.; Soto, C. *Curr. Med. Chem.* **2002**, *9*, 963.
17. Asada, H.; Douen, T.; Waki, M.; Adachi, S.; Fujita, T.; Yamamoto, A.; Muranishi, S. *J. Pharm. Sci.* **1995**, *84*, 682.
18. Wong, A. K.; Ross, B. P.; Chan, Y. N.; Artursson, P.; Lazorova, L.; Jones, A.; Toth, I. *Eur. J. Pharm. Sci.* **2002**, *16*, 113.
19. Futaki, S.; Goto, S.; Sugiura, Y. *J. Mol. Recognit.* **2003**, *16*, 260.
20. Toth, I.; Malkinson, J. P.; Flinn, N. S.; Drouillat, B.; Horvath, A.; Erchegyi, J.; Idei, M.; Venetianer, A.; Artursson, P.; Lazorova, L.; Szende, B.; Keri, G. *J. Med. Chem.* **1999**, *42*, 4010.
21. Egleton, R. D.; Mitchell, S. A.; Huber, J. D.; Janders, J.; Stropova, D.; Polt, R.; Yamamura, H. I.; Hruby, V. J.; Davis, T. P. *Brain Res.* **2000**, *881*, 37.
22. Hadley, M. E.; al-Obeidi, F.; Hruby, V. J.; Weinrach, J. C.; Freedberg, D.; Jiang, J. W.; Stover, R. S. *Pigment Cell Res.* **1991**, *4*, 180.
23. al-Obeidi, F.; Hruby, V. J.; Yaghoubi, N.; Marwan, M. M.; Hadley, M. E. *J. Med. Chem.* **1992**, *35*, 118.

24. Todorovic, A.; Holder, J. R.; Bauzo, R. M.; Scott, J. W.; Kavanagh, R.; Abdel-Malek, Z.; Haskell-Luevano, C. *J. Med. Chem.* **2005**, *48*, 3328.
25. Taylor, F. R.; Wen, D.; Garber, E. A.; Carmillo, A. N.; Baker, D. P.; Arduini, R. M.; Williams, K. P.; Weinreb, P. H.; Rayhorn, P.; Hronowski, X.; Whitty, A.; Day, E. S.; Boriack-Sjodin, A.; Shapiro, R. I.; Galdes, A.; Pepinsky, R. B. *Biochemistry* **2001**, *40*, 4359.
26. Schwyzer, R. *Biochemistry* **1986**, *25*, 4281.
27. Sargent, D. F.; Schwyzer, R. *Proc. Natl. Acad. Sci. U.S.A.* **1986**, *83*, 5774.
28. Anderson, G. P.; Linden, A.; Rabe, K. F. *Eur. Respir. J.* **1994**, *7*, 569.
29. Gres, M. C.; Julian, B.; Bourrie, M.; Meunier, V.; Roques, C.; Berger, M.; Boulenc, X.; Berger, Y.; Fabre, G. *Pharm. Res.* **1998**, *15*, 726.
30. Artursson, P.; Karlsson, J. *Biochem. Biophys. Res. Commun.* **1991**, *175*, 880.
31. Rubas, W.; Jezyk, N.; Grass, G. M. *Pharm. Res.* **1993**, *10*, 113.
32. Stewart, B. H.; Chan, O. H.; Lu, R. H.; Reyner, E. L.; Schmid, H. L.; Hamilton, H. W.; Steinbaugh, B. A.; Taylor, M. D. *Pharm. Res.* **1995**, *12*, 693.
33. Artursson, P.; Palm, K.; Luthman, K. *Adv. Drug Delivery Rev.* **2001**, *46*, 27.
34. *Fmoc Solid-Phase Peptide Synthesis: A Practical Approach*; Chan, W.C., White, P.D., Eds.; Oxford University Press, 2000.
35. Barde, Y. A.; Edgar, D.; Thoenen, H. *Proc. Natl. Acad. Sci. U.S.A.* **1980**, *77*, 1199.
36. Dunnett, C. W. *J. Am. Stat. Assoc.* **1955**, *50*, 1096.
37. Bonferroni, C. E. *Pubblicazioni del R Istituto Superiore di Scienze Economiche e Commerciali di Firenze* **1936**, *8*, 3.
38. Bolin, D. R.; Swain, A. L.; Sarabu, R.; Berthel, S. J.; Gillespie, P.; Huby, N. J.; Makofske, R.; Orzechowski, L.; Perrotta, A.; Toth, K.; Cooper, J. P.; Jiang, N.; Falcioni, F.; Campbell, R.; Cox, D.; Gaizband, D.; Belunis, C. J.; Vidovic, D.; Ito, K.; Crowther, R.; Kammlott, U.; Zhang, X.; Palermo, R.; Weber, D.; Guenot, J.; Nagy, Z.; Olson, G. L. *J. Med. Chem.* **2000**, *43*, 2135.
39. Youdim, K. A.; Avdeef, A.; Abbott, N. J. *Drug Discovery Today* **2003**, *8*, 997.
40. Artursson, P.; Palm, K.; Luthman, K. *Adv. Drug Delivery Rev.* **1996**, *22*, 67.